

OPEN REGULATORY NETWORKS AND MODULARITY

R. LIMA, A. MEYRONEINC & E. UGALDE

Centre de Physique Théorique, CNRS–Luminy Case 907, 13288 Marseille Cedex 09, France, lima@cpt.univ-mrs.fr

Departamento de Matemáticas, Instituto Venezolano de Investigaciones Científicas, Apartado 21827, Caracas 1020A, Venezuela, ameyrone@ivic.ve

Instituto de Física, Universidad Autónoma de San Luis Potosí, Av. Manuel Nava 6, San Luis Potosí, 78290 México, ugalde@ifisica.uaslp.mx

ABSTRACT. We study the dynamical properties of small regulatory networks treated as non autonomous dynamical systems called *modules* when working inside larger networks or, equivalently when subject to external signal inputs. Particular emphasis is put on the interplay between the internal properties of the open systems and the different possible inputs on them to deduce new functionalities of the modules. We use discrete–time, piecewise–affine and piecewise–contracting models with interactions of a regulatory nature to perform our study.

Keywords: Regulatory Dynamics on Networks, Open Systems, Motifs, Modularity.

MSC: 37N25, 37L60, 05C69.

1. INTRODUCTION

The structure of genetic regulatory networks can be abstracted by directed graphs, where the nodes represent genes and the arrows (oriented edges) stand for their interactions through transcription/translation products. These interactions may be either activations or inhibitions. Given the large number of components in most networks of biological interest, connected by positive and negative feedback loops, the comprehension of the dynamics of a system is often difficult if not impossible. In this context, *mathematical modeling* eventually supported by *computer tools* can contribute to the analysis of a regulatory network by allowing the biologist to focus on a restricted number of plausible hypotheses, or to easily read some observed features of the system. We refer to [2, 8] and references therein for an account of the huge and still growing literature on this topic.

It has been evidenced that the existence of network *motifs*, a set of recurring patterns inside large biological regulatory networks, shall give new insight on the understanding of the performances of the global network. We refer to the review [3] (see also [2]) for a clear and complete description of such a point of view and references therein for recent work in different specific biological contexts. Since most of the time these *modules* [19] also have input and output interactions relating to the rest of the network, they may be considered as open

dynamical systems, meaning distinguished parts of larger 'closed' systems, the remaining of the network being an 'environment'.

In the classical literature of Dynamical Systems, "open" or "forced" dynamical systems are defined as those for which the dynamics depends on internal rules as well as on inputs from the environment, then producing some outputs back to the environment. The notion of open systems is also the groundwork of System Theory and many results concerning the possibility to control linear and nonlinear systems have been obtained in the last decades [20, 13]. Here we are interested in a description of the dynamics of these systems in all the parameter space and subjected to any external signal.

When comparing these modules with the standard corresponding regulatory networks we are faced to new questions to understand their dynamical behavior and, therefore, their possible new functionalities. Here we study some of these questions by searching first for general properties of such systems and by trying to identify the fundamental mechanisms at work in the open systems we deal with. Although our definition of module is not the most general possible, as it will appear next, it seems that it contains all the cases treated in the literature and, remarkably, it allows simpler proofs in many cases.

These general properties must be complemented in each particular case with further analysis to derive additional specific properties of a given module and we perform this task for some examples.

What we found in the general case may be summarized as follows: each elementary input selects a particular subset of the phase space and a particular dynamical rule among a (finite) set of possibilities allowed by the module; therefore any (finite or infinite) sequence of inputs drives the dynamics of the module along a pre-determined maze of possible paths. Simple sequences of inputs give rise to simple dynamics of the module and therefore to simple responses (outputs), but, since they fix the system in a "corner" of its phase space, the system may acquire new functionalities as we shall see in some examples. Moreover, because such constraints in phase space may depend of the values of the parameters of the system and not only of its structure (the pattern of interactions) it turns out that the structure cannot determine the functionality in all cases [12]. It will also be clear from what follows that, on the contrary, in some cases it can happen that the type of response is not essentially affected by a change of parameters, and only particular aspects do, *e. g.* speeding or slowing of the response. Interestingly, when a module can perform more than one function, each one is generally robustly provided. This fact does not exclude the possibility of a fine tuning of the interaction between the input and the internal dynamics that may end in an interesting interplay between both.

Despite the fact that the proofs of our results is done for a special type of model of regulatory networks, i. e. discrete time dynamical systems [8, 6, 14, 25], we believe that these results have a more general thrust, for the underlying mechanisms are common to other types of dynamical systems, as ODEs for instance.

Besides, discrete-time models provide a simple framework where the consequences of interaction delays are already included and they largely benefit from tools and techniques in the Dynamical Systems theory [8, 6].

We study two different types of modules. The first one, called regulatory cascades (RC), is defined as any open network without (internal) circuits. The second type, called forced circuits (FC), is any open circuit. The general case can be build as a combination of such elementary pieces and at the end we sketch the analysis of one such mixed RC-FC module on the bases of our previous results.

For the RC modules we give a complete description of the dynamics. We specify, in particular, the output as a function of the input knowing the structure and the internal set of parameters of the module. It turns out that the dynamics of such RC works as a special kind of cellular automata and, due to a celebrated result in [15], they can emulate a Universal Turing Machine!

For the FC modules, we give a complete description of the dynamics for the cases of one and two units in the fundamental case of constant inputs and for all the parameter values of the circuits. Using the exponential contracting rate of the system, the behavior for more general input signals follows. Here the input level fixes the dynamics of the module in a subset of the phase space allowing dynamical regimes that do not correspond to the typical autonomous version.

The relation between the transducer like point of view used in the RC analysis and the constrained phase space used for the FC is done by symbolic dynamics.

It is worth to notice that, as we shall see, modules that we show to perform different dynamical behaviors may be functionals in different situations [16], therefore allowing to perform different functions either for given values of parameters through different inputs, or vice-versa.

The paper is organized as follows: section 2 recalls the basic properties of the models, section 3 describes the dynamics of the regulatory cascades (RC), section 4 describes the dynamics of the forced circuits (FC) and section 5 shows how, in simple cases, it is possible to treat a mixed type module. Section 6 is concerned with final comments and outlooks.

2. DESCRIPTION OF THE MODEL AND GENERAL PROPERTIES

2.1. Discrete-time regulatory networks.

We consider a special class of models, i. e. discrete-time regulatory networks. These are discrete-time dynamical systems on a network (see [8, 25, 14, 6]). By a network we mean a digraph, with vertices in a given finite set V and with arrows (oriented links) taken from another given finite set $A \subseteq V \times V$, together with a set of additional characteristics we introduce next.

Vertices account for interacting units carrying a certain activity level (a scalar in $[0, 1]$ associated to each unit $v \in V$), depicting the product of a gene, and the arrows account for the interactions between them.

Although the results presented below hold for more general interactions (as for instance multiplicative interactions) we restrict ourselves to additive inhibitory-activating interactions for the sake of simplicity (see [25, 14, 6]).

The model is defined as follows: to each arrow $(u, v) \in A$ we associate an interaction threshold $T_{uv} \in [0, 1]$, a sign $\sigma_{uv} \in \{-1, 1\}$ indicating whether the action of u over v is an activation ($\sigma_{uv} = 1$) or is an inhibition ($\sigma_{uv} = -1$), and a coupling strength $\kappa_{uv} \in [0, 1]$. The activity level of the network at time $t \in \mathbb{N}$ is specified by the collection of the $\mathbf{x}_v^t \in [0, 1]$, expressing the activity of each unit $v \in V$ at time $t \in \mathbb{N}$.

Denoting $I(v) := \{u \in V : (u, v) \in A\}$ the set of vertices acting over a vertex $v \in V$, the activation at time $t + 1$ of the unit $v \in V$ is given by

$$(1) \quad \mathbf{x}_v^{t+1} := a\mathbf{x}_v^t + (1 - a) \sum_{u \in I(v)} \kappa_{uv} H(\sigma_{uv}(\mathbf{x}_u^t - T_{uv})).$$

The constant $a \in [0, 1)$ appearing in the equation plays the role of a degradation rate. In absence of interaction, the activity level of a unit v decreases exponentially fast to zero, $\mathbf{x}_v^t = a^t \mathbf{x}_v^0$. In the interaction terms, H represents the Heaviside (step) function, $H(x) = 1$ for $x > 0$ and $H(x) = 0$ for $x \leq 0$. Hence each interaction term is a piecewise constant function whose value changes whenever one of the coordinates \mathbf{x}_u^t crosses its own threshold T_{uv} .

Without loss of generality the coupling strengths are normalized by $\sum_{u \in I(v)} \kappa_{uv} = 1$ for each $v \in V$.

In [6] we described the dynamics of some of this networks in great details. We shall come back to these results when comparing with their open versions.

2.2. Open networks.

As mentioned above an open network is defined as part of a larger regulatory network together with the corresponding incoming and outgoing arrows, respectively from and to the rest of the network. *Motifs* are such open networks that appear more often than the expected frequency in some null statistical graph model [17, 3]. In the present paper we study open subnetworks without any reference to their possible abundance inside a larger regulatory network and we rather call "module" any ('simple') open subnetwork.

Any collection of N vertices $V_{\text{mod}} \subsetneq V$ of a network V defines an open network (as long as not all the arrows with head in V_{mod} have tail in V_{mod}).

Formally an *open regulatory network* or a *module* is a regulatory network with vertices $V_{\text{mod}} \subsetneq V$, the internal units, and three kind of distinguished arrows:

- (1) the incoming arrows, denoted A_{in} is the set $\{(u, v) : u \in V \setminus V_{\text{mod}}, v \in V_{\text{mod}}\}$,
- (2) the inner arrows denoted A_{mod} is the set $\{(u, v) : u \in V_{\text{mod}}, v \in V_{\text{mod}}\}$ and,
- (3) the outgoing arrows denoted A_{out} the set $\{(u, v) : u \in V_{\text{mod}}, v \in V \setminus V_{\text{mod}}\}$.

The dynamics of the module is defined using the same rule (see Eq. 1) as for the general case. However, as we consider the module as an open system (as if there were no feedback loops from V_{mod} to V_{mod} through $V_{\text{ext}} := V \setminus V_{\text{mod}}$) we may replace the exact knowledge of \mathbf{x}_u^t for $u \in V_{\text{ext}}$ by the one of the corresponding symbol: $\theta_{uv}^t := H(\sigma_{uv}(\mathbf{x}_u^t - T_{uv}))$.

Therefore, the state of the system at a given time $t \in \mathbb{N}$ is determined by a vector $\mathbf{x}^t \in [0, 1]^{\#V_{\text{mod}}}$ and the imposed external activation levels θ_{uv}^t for all $(u, v) \in A_{\text{in}}$. We refer to the array of external activations, $\{\theta_{uv}^t \text{ for all } (u, v) \in A_{\text{in}}\}$, as the *input code* θ_{in}^t .

In the case of an open system, the evolution rule (1) reads:

$$(2) \quad \mathbf{x}_v^{t+1} := a\mathbf{x}_v^t + (1-a)D_v(\mathbf{x}^t, \theta_{\text{in}}^t)$$

with

$$(3) \quad D_v(\mathbf{x}^t, \theta_{\text{in}}^t) := \sum_{u \in I(v) \cap V_{\text{mod}}} \kappa_{uv} H(\sigma_{uv}(\mathbf{x}_u^t - T_{uv})) + \sum_{u \in I(v) \cap V_{\text{ext}}} \kappa_{uv} \theta_{uv}^t$$

The state of the internal units determine the activation of the internal arrows A_{mod} .

We put together this data in the internal code

$$(4) \quad \theta_{\text{mod}}^t := (H(\sigma_{uv}(\mathbf{x}_u^t - T_{uv})) : (u, v) \in A_{\text{mod}}).$$

Finally, the influence of the open subnetwork $(V_{\text{mod}}, A_{\text{mod}})$ over its environment is codified in the sequences of output activations, which we group in *the output code*

$$(5) \quad \theta_{\text{out}}^t := (H(\sigma_{uv}(\mathbf{x}_u^t - T_{uv})) : (u, v) \in A_{V_{\text{mod}} \rightarrow V_{\text{ext}}}).$$

In Figure 1 we give an example of a module together with its external complement.

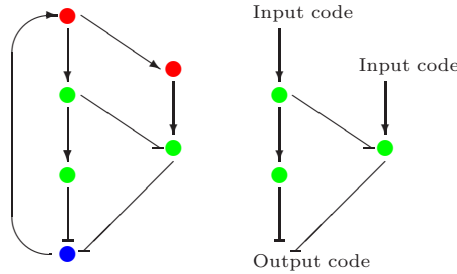


FIGURE 1. Open subnetwork (green) extracted from a larger one (red, green and blue). Hammer-like arrows represent inhibitory interactions, standard arrows activatory ones.

From Equations (2) and (3), we see that each possible input code $\theta := \theta_{\text{in}}$ uniquely determines an affine contraction $F_\theta : [0, 1]^{\#V_{\text{mod}}} \rightarrow [0, 1]^{\#V_{\text{mod}}}$ given by

$$(6) \quad F_\theta(\mathbf{x}) = a\mathbf{x} + (1-a)D_v(\mathbf{x}, \theta_{\text{in}}).$$

The collection of all these affine contractions defines an iterated function system (IFS)

$$(7) \quad \mathcal{F} := \left\{ F_\theta : [0, 1]^{\#V_{\text{mod}}} \rightarrow [0, 1]^{\#V_{\text{mod}}} : \theta \in \{0, 1\}^{\#A_{\text{in}}} \right\},$$

from where the dynamics reads:

$$(8) \quad \mathbf{x}^{t+1} = F_{\theta_{t-1}} \circ \dots \circ F_{\theta_0}(\mathbf{x}^0),$$

with attractor

$$(9) \quad \Omega_{\mathcal{F}} := \bigcap_{t \geq 0} \bigcup_{\theta^0 \dots \theta^{t-1} \in (\{0,1\}^{\#A_{\text{in}}})^t} F_{\theta^{t-1}} \circ \dots \circ F_{\theta^0}([0, 1]),$$

Remark 2.1. The form in Equation (3) is not the most general for which the results below can be proved. Notice however that by a proper choice of the internal and external thresholds it already includes the cases of the AND and OR logical outputs [3]. On the other hand, the essential ingredient needed for all the proofs is the collection of affine contractions indexed by the possible forcing codes, defining an iterated function system (IFS) as in (7) and (8). It is also well known that such IFS are skew product dynamical systems [4]. However, because in our case we are interested in properties of very specific models, known results about the latter systems are only used to fix the general context of our study. They are, in particular, implicitly used when arguing on the genericity of some properties proved below.

In fact, for discrete-time regulatory networks, there is a way to understand the dynamics of an open system in terms of a collection of autonomous mirror systems. For an open system $(V_{\text{mod}}, A_{\text{mod}}, A_{\text{in}})$ and any constant forcing code: $\theta^0 \dots \theta^t \dots$, with $\theta^t = \theta \forall t \in \mathbb{N}$, let Ω_{θ} be the corresponding attractor, named *basic attractor* and defined by Equation (9). Now, for each constant forcing code, the system will evolve inside an invariant subset of its phase space as an autonomous system, up to an affine change of variables. This invariant subset attracts all the trajectories starting outside. The last correspond, by the same change of variables, to those starting outside $[0, 1]$ in the closed system and for which the behavior is known [6].

On the other hand, the attractors for the closed systems, and therefore for each constant forcing of the open system, are unions of the so called *global* orbits, those that can be extended backward in time up to $-\infty$ inside $[0, 1]^{\#V_{\text{mod}}}$ (see [6]). The same is then true for every basic attractor of the open system. The generic case, in measure sense in parameter space, is such that each of the basic attractors is uniformly bounded away from the discontinuities (the internal thresholds). In this case, any orbit with constant forcing will approach the attractor exponentially fast, with rate $\log a$. Therefore, for a general forcing the corresponding orbit will wander around the basic attractors and will closely approach one if the forcing input stays constant during a sufficiently long duration, and the dynamical behavior of the system is clear in this case. Moreover it tells us that a is the main parameter controlling how fast the system respond to a new input signal. This suggest that a may be experimentally estimated when the corresponding proteins are not actively degraded, as it is the case for most proteins in growing bacterial cells [3].

For the remainder exceptional cases of the parameter values, the attractor will be arbitrarily close to the discontinuities. In this situation an orbit approaching a basic attractor will sometimes be close but on the opposite side of the attractor. This will cause an accident in the internal code followed by an unforeseeable length of time before the orbit to approach again the basic attractor.

The rigorous description of the dynamics of all the possible internal codes of the attractor in this case is still an open mathematical problem.

Recall that a path in a network (V, A) is a sequence of vertices $(v_0, v_1, \dots, v_{\ell-1})$, such that $(v_i, v_{i+1}) \in A$ for $0 \leq i \leq \ell-2$. If in addition $(v_{\ell-1}, v_0) \in A$, then we said that $(v_0, v_1, \dots, v_{\ell-1})$ is a cycle. Circuits are cycles with no repeating vertices.

3. REGULATORY CASCADES

3.1. Description of the regulatory cascade.

Among the open structures encountered in the analysis of biological networks, and that could be associated to certain functions, are the feed-forward loops, the dense overlapping regulons, and the diamonds (see [3]). These motifs have a two-common feature once regarded as digraphs: (a) they are connected and (b) they do not contain cycles. As mentioned in the introduction, and as we will show below, open sub-systems on these kind of networks behave as finite state translators, from the input to the output code, with a certain delay which in principle may depend on the input structure.

A *regulatory cascade (RC)* is an open subsystem $(V_{\text{mod}}, A_{\text{mod}})$ defined in a regulatory network, such that it is connected and with no cycles. It is clear that such a network cannot be strongly connected. The open subnetwork in Figure 1 is an example.

The simplest RC (see Figure 2) consists of a single internal vertex $v \in V$, forced by vertices $U := \{u_1, \dots, u_n\} \subset V_{\text{ext}} \equiv V \setminus \{v\}$, and affecting a collection of vertices $W := \{w_1, \dots, w_m\} \subset V_{\text{ext}}$. Its functioning can be thought as the translation of an input code $\theta_{\text{in}}^t := (H(\sigma_{uv}(\mathbf{x}_u^t - T_{uv})) : u \in U)$, into an output code $\theta_{\text{out}}^t := (H(\sigma_{vw}(\mathbf{x}_v^t - T_{vw})) : w \in W)$. We assume that the vertex v does not interact with itself, so that $(v_0, v_0) \notin A$. We will refer to this open subsystem as the *elementary transducer (ET)*.

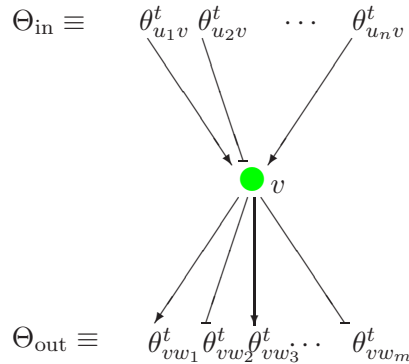


FIGURE 2. The elementary transducer: an open subsystem consisting of a single vertex with several input and output arrows. Lines with hammer-like heads represent inhibitory interactions, arrows activatory ones.

Another elementary regulatory cascade is what we call a *regulatory chain RCh*. It is defined over a linear network $\rightarrow v_1 \rightarrow \dots \rightarrow v_n \rightarrow$ consisting of a path connecting the input vertex (v_1) to the output one (v_n), with input and output arrows, (u, v_1) and (v_n, w) respectively. Since to each interaction mode (activation/inhibition) it corresponds a sign (+1/-1), we can therefore associate the sign $\sigma := \prod_{k=1}^{n-1} \sigma_{v_k v_{k+1}} \times \sigma_{v_n w}$ to the RCh $\rightarrow v_1 \rightarrow \dots \rightarrow v_n \rightarrow$. As we will show below, the functioning of this chain as a transducer essentially depends of its sign.

A remarkable family of RCs are the so called *feedforward loops (FFL)*, consisting of three internal vertices connected as indicated in Figure 3. There are single input and output arrows, and two chains (elementary paths) connecting them. Taking this into account, the feedforward loops were classified as coherent and incoherent, depending on whether the sign of the chains composing them are of the same or opposite signs (see [3] for details).

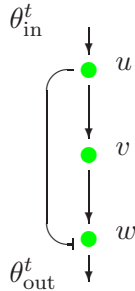


FIGURE 3. Incoherent feedforward loop of the type 3

As we will show below, it is convenient to decompose a given regulatory cascade into elementary transducers and regulatory chains.

3.2. Dynamics of the regulatory cascade.

We investigate how efficiently and robustly a regulatory cascade can work when transmitting information. Two mathematical questions are clearly related to this: what is the time length of the external signal needed by the cascade system to tie an output, and what is the possible dependence of the output on the internal state of the cascade at the time when the input is detected. In particular, our aim in this section is to determine the conditions under which each output code of a RC depends only on the sequence of input codes received during a finite period of time, whose length depends on the structure and on the parameters of the RC. When this phenomenon occurs we say that the cascade resolves the output code with a finite delay. To this aim, we will first analyze in details the simplest RC, i. e. the elementary transducer. Since every RC can be decomposed into a collection of ET's, the conditions under which a general regulatory cascade resolves the code, and is functioning as a code transducer, will be deduced from the behavior of its elementary transducers.

3.2.1. The elementary transducer.

For the ET in Figure 2, a temporal sequence of input codes $\Theta_{\text{in}} := (\theta_{\text{in}}^t)_{t \in \mathbb{N}}$, completely determines the evolution of the internal vertex:

$$(10) \quad \mathbf{x}_v^{t+1} := a\mathbf{x}_v^t + (1-a) \sum_{u \in U} \kappa_{uv} \theta_{uv}^t.$$

Hence, the temporal sequence of output code $\Theta_{\text{out}} := (\theta_{\text{out}}^t)_{t \in \mathbb{N}}$ can be computed from this sequences of input codes and the initial condition \mathbf{x}_v^0 .

When the input signal has been present for an infinite time, the output code depends only on the infinite sequence of input signals. Otherwise, if the input signal started its action at time t_0 , then the output code will also depend on $\mathbf{x}_v^{t_0}$, the activity level of the internal vertex at time t_0 .

According to Equation (10), from a sequence of input codes $\Theta_{\text{in}} := (\theta_{\text{in}}^\tau)_{\tau=t_0}^t$, and an initial condition $\mathbf{x}_v^{t_0}$, we obtain

$$(11) \quad \mathbf{x}_v^t = a^{t-t_0} \mathbf{x}_v^{t_0} + (1-a) \sum_{\tau=t_0}^{t-1} a^{t-\tau-1} \left(\sum_{u \in U} \kappa_{uv} \theta_{uv}^\tau \right),$$

from which we compute the output code $\theta_{\text{out}}^t := (H(\sigma_{vw}(\mathbf{x}_v^t - T_{vw})) : (v, w) \in A_{\text{out}})$. Hence, in order to compute the temporal sequence of output codes $\Theta_{\text{out}} := (\theta_{\text{out}}^t)_{t \in \mathbb{N}}$, we have to determine the position of \mathbf{x}_v^t with respect to the output thresholds $\{T_{vw} : (v, w) \in A_{\text{out}}\}$, and so for each time $t \in \mathbb{N}$. To solve this problem we take into account the following.

1.- The internal vertex IFS. Each possible input code $\theta_{\text{in}} := (\theta_{uv} : (u, v) \in A_{\text{in}})$, uniquely determines an affine contraction $F_\theta : [0, 1] \rightarrow [0, 1]$ given by

$$(12) \quad F_\theta(\mathbf{x}) = a\mathbf{x} + (1-a) \sum_{(u,v) \in A_{\text{in}}} \kappa_{uv} \theta_{uv}.$$

As already mentioned, the collection of all these affine contractions defines the iterated function system (IFS)

$$(13) \quad \mathcal{F} := \left\{ F_\theta : [0, 1] \rightarrow [0, 1] : \theta \in \{0, 1\}^{\#A_{\text{in}}} \right\},$$

with attractor

$$(14) \quad \Omega_{\mathcal{F}} := \bigcap_{t \geq 0} \bigcup_{\theta^0 \dots \theta^{t-1} \in \{0, 1\}^{\#A_{\text{in}}}^t} F_{\theta^{t-1}} \circ \dots \circ F_{\theta^0}([0, 1]).$$

2.- Resolution of the output code. For each input sequence $(\theta_{\text{in}}^\tau)_{\tau \geq 0}$ and all time $t \geq 1$, let $I_{\theta_{\text{in}}^0 \dots \theta_{\text{in}}^{t-1}} := F_{\theta_{\text{in}}^{t-1}} \circ \dots \circ F_{\theta_{\text{in}}^0}([0, 1])$. The evolution of \mathbf{x}_v^t is such that for each $t_0 \in \mathbb{N}$ fixed and all $t \geq t_0$ we have

$$\mathbf{x}_v^t \in I_{\theta_{\text{in}}^0 \dots \theta_{\text{in}}^{t-1}} \subset I_{\theta_{\text{in}}^{t-t_0} \dots \theta_{\text{in}}^{t-1}} \equiv [\mathbf{x}_v(\theta_{\text{in}}^{t-t_0} \dots \theta_{\text{in}}^{t-1}), a^{t_0} + \mathbf{x}_v(\theta_{\text{in}}^{t-t_0} \dots \theta_{\text{in}}^{t-1})],$$

where

$$(15) \quad \mathbf{x}_v(\theta_{\text{in}}^{t-t_0} \dots \theta_{\text{in}}^{t-1}) := (1-a) \sum_{\tau=t-t_0}^{t-1} a^{t-\tau-1} \left(\sum_{u \in U} \kappa_{uv} \theta_{uv}^\tau \right).$$

the t_0 approximation to the activity level. From Equation (15) it readily follows that

$$|\mathbf{x}_v^t - \mathbf{x}_v(\theta_{\text{in}}^{t-t_0} \dots \theta_{\text{in}}^{t-1})| \leq a^{t_0},$$

for all $t > t_0$. Hence, for each t_0 fixed, the output code can be resolved for all the input codes $\theta_{\text{in}}^{t-t_0} \dots \theta_{\text{in}}^{t-1}$ satisfying

$$\min_{w \in W} |\mathbf{x}_v(\theta_{\text{in}}^{t-t_0} \dots \theta_{\text{in}}^{t-1}) - T_{uw}| > a^{t_0}.$$

As mentioned above, in this case we say that the code is resolved with a finite delay t_0 . The set of input code sequences which can be resolved with a delay t_0 grows exponentially with t_0 . Depending on the parameters of the system, the complement of this set could grow exponentially as well.

There are two cases where we can show that the ET resolves the input code in a finite time. The first case relies on an internal characteristic of the ET we call *internal separability*. In this case, with probability 1, the thresholds are separated from the attractor. In the second case we assume that the input signal satisfies a property we name *low input complexity*.

3.- Internal separability. A possible simplification occurs when the attractor $\Omega_{\mathcal{F}}$ is a Cantor set. This is the case if in Equation (12) the contraction rate a is sufficiently small. In this cantorian case, for any $T \notin \Omega_{\mathcal{F}}$ there exists a *depth* $t_T \in \mathbb{N}$ such that $T \notin \bigcup_{\theta^0 \dots \theta^{\tau-1} \in (\{0,1\}^{\#A_{\text{in}}})^\tau} I_{\theta_{\text{in}}^0 \dots \theta_{\text{in}}^{\tau-1}}$, for each $\tau \geq t_T$. Hence, if $\{T_{vw} : (v, w) \in A_{\text{out}}\} \cap \Omega_{\mathcal{F}} = \emptyset$, which happens with probability 1, the maximal depth $t_0 := \max_T t_T$ is such that $\theta_{\text{out}}^t = (H(\sigma_{vw}(\mathbf{x}_v(\theta_{\text{in}}^{t-t_0} \dots \theta_{\text{in}}^{t-1}))) : (v, w) \in A_{\text{out}})$. In this case the elementary transducer acts as a cellular automata, transforming sequences of input codes to sequences of output ones, with a delay t_0 . Indeed, we can define $\Phi : (\{0,1\}^{\#A_{\text{in}}})^{\mathbb{N}} \rightarrow (\{0,1\}^{\#A_{\text{out}}})^{\mathbb{N}}$, such that

$$(16) \quad \Phi(\theta_{\text{in}})_\tau := (H(\sigma_{vw}(\mathbf{x}_v(\theta_{\text{in}}^{t-t_0} \dots \theta_{\text{in}}^{t-1}))) : w \in W) = \theta_{\text{out}}^{\tau+t_0},$$

with $\mathbf{x}_v(\theta_{\text{in}}^{t-t_0} \dots \theta_{\text{in}}^{t-1})$ the t_0 approximation to the activity level defined in Equation (15). Let us emphasize that in the cantorian case, the condition $\{T_{vw} : (v, w) \in A_{\text{out}}\} \cap \Omega_{\mathcal{F}} = \emptyset$ holds with probability 1 with respect to Lebesgue, i. e. a cantorian ET typically operates as a cellular automata. If so is the case, we say that the ET satisfies internal separability. If on the contrary $\{T_{vw} : w \in W\} \cap \Omega_{\mathcal{F}} \neq \emptyset$, there would be for each $t \in \mathbb{N}$ input codes $(\theta_{\text{in}}^0 \dots \theta_{\text{in}}^{t-1})$ that cannot be resolved in finite time.

Example 3.1. Let us illustrate the functioning of the elementary transducer in the internally separable case. Consider an ET with two input arrows (u_1, v) and (u_2, v) , with coupling constants $\kappa_{u_1 v} = 1 - \kappa_{u_2 v} = 2/3$, and a single output arrow (v, w) , as shown in Figure 4. Let $T_{v,w} = 83/150$ and $\sigma_{vw} = -1$. Fix the contraction rate $a = 1/5$. In this case the associated IFS is

$$\mathcal{F} := \{F_{00}(\mathbf{x}) = \mathbf{x}/5, F_{01}(\mathbf{x}) = \mathbf{x}/5 + 4/15, F_{10}(\mathbf{x}) = \mathbf{x}/5 + 8/15, F_{11}(\mathbf{x}) = \mathbf{x}/5 + 4/5\}.$$

Its attractor $\Omega_{\mathcal{F}}$ is a Cantor set of box dimension $d_{\text{box}}(\Omega_{\mathcal{F}}) = \log(4)/\log(5)$. In this particular case, the third approximant $\bigcup_{\theta_{\text{in}}^0 \theta_{\text{in}}^1 \theta_{\text{in}}^2 \in (\{0,1\}^{\#U})^3} I_{\theta_{\text{in}}^0 \theta_{\text{in}}^1 \theta_{\text{in}}^2}$ of the IFS's attractor is the disjoint union of 64 closed intervals of length $1/125$, indexed by codes in $(\{0,1\}^2)^3$. None of these 64 intervals contain the output threshold, therefore we have a depth $t_0 = 3$ in this case.

The translating cellular automata $\Phi(\{0, 1\}^2)^{\mathbb{N}} \rightarrow \{0, 1\}^{\mathbb{N}}$ is defined in this case by the local function $\phi : (\{0, 1\}^2)^3 \rightarrow \{0, 1\}$ such that

$$\phi(\theta_{\text{in}}^0 \theta_{\text{in}}^1 \theta_{\text{in}}^2) = \begin{cases} 1 & \text{if } \theta_{\text{in}}^0 \in \{00, 01\} \text{ or } \theta_{\text{in}}^0 \theta_{\text{in}}^1 \theta_{\text{in}}^2 \in \{(10, 00, 00), (10, 00, 01)\}, \\ 0 & \text{otherwise.} \end{cases}$$

Here, for instance, all input sequences in $\{11, 01\}^{\mathbb{N}}$ produce the same output sequence $000 \dots$.

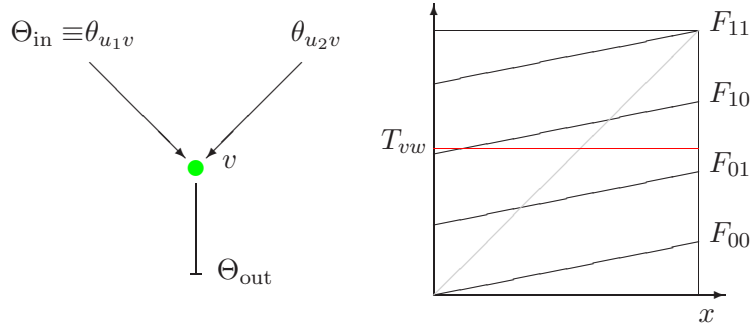


FIGURE 4. The elementary transducer of Example 3.1 and its associated IFS.

4.- Low input complexity. The attractor $\Omega_{\mathcal{F}}$ is a Cantor set if and only if $\bigcup_{\theta \in \{0,1\}^{\#A_{\text{in}}}} F_{\theta}([0, 1]) \subsetneq [0, 1]$. When on the contrary $\bigcup_{\theta \in \{0,1\}^{\#A_{\text{in}}}} F_{\theta}([0, 1])$ covers $[0, 1]$, even if the number of input codes that can be resolved with a delay t_0 grows exponentially fast with t_0 , the cardinality of its complement could also grow exponentially fast. In this case, in order to resolve the output code in finite time, we consider a particular class of input sequences.

The *temporal complexity* of a sequence of input codes $\Theta_{\text{in}} \equiv (\theta_{\text{in}}^t)_{t \geq 0}$ is defined as

$$(17) \quad C_{\Theta_{\text{in}}}(t) \equiv \# \{ \theta_{\text{in}}^{\tau} \dots \theta_{\text{in}}^{\tau+t} : \tau \in \mathbb{N} \}.$$

If the sequence of input codes Θ_{in} is such that for a fixed $k \in \mathbb{N}$ and all t sufficiently large, $C_{\Theta_{\text{in}}}(t) \leq t^k$ (in this case we say that the sequences of input codes have polynomial complexity), then the output code can be typically resolved with a finite delay. We are interested in the polynomial case due to the fact that strongly contractive regulatory networks produce sequences of codes with polynomial complexity [14]. We conjecture that in all cases the sequences of codes produced by a regulatory network have polynomial complexity.

We state our result in this case as follows. For sequences of input codes Θ_{in} satisfying $C_{\Theta_{\text{in}}}(t) \leq t^k$ for a fixed $k \in \mathbb{N}$ and all t sufficiently large, then, with probability 1 in the output thresholds, there exists a fixed delay time $t_1 \geq t_0$ such that

$$\theta_{\text{out}}^t = (H(\sigma_{vw}(\mathbf{x}_v(\theta_{\text{in}}^{t-t_1} \dots \theta_{\text{in}}^{t-1}))) : w \in W),$$

with $\mathbf{x}_v(\theta_{\text{in}}^{t-t_1} \dots \theta_{\text{in}}^{t-1})$ as defined by (15). The ET typically functions as a cellular automata when restricted to sequences of input codes with polynomial complexity. In this case we say that the system has low input complexity.

Remark 3.1. The behavior of any totalistic cellular automaton can be obtained from an internally separable ET. Since totalistic cellular automata can simulate any Turing machine [11], it follows that ET's have universal computing capabilities.

3.2.2. The Regulatory Chain (RCh).

As mentioned above, a regulatory chain is an open regulatory network defined over a linear digraph $\rightarrow v_1 \rightarrow \dots \rightarrow v_n \rightarrow$, connecting the input vertex (v_1) to the output one (v_n), with input and output arrows (u, v_1) and (v_n, w) respectively. To this chain we associate the sign $\sigma := \prod_{k=1}^{n-1} \sigma_{v_k v_{k+1}} \times \sigma_{v_n w}$. The functioning of this chain as a transducer essentially depends of this sign.

We have two possibilities depending on the common contraction rate $a \in [0, 1)$. The simplest one occurs when $a < 1/2$, in which case all the vertices v_1, \dots, v_n considered as elementary transducers typically act as a cellular automata. Indeed, if $a < 1/2$ to each vertex we associate the same dyadic IFS

$$(18) \quad \mathcal{F}_{\text{dyadic}} := \{F_\theta : [0, 1] \rightarrow [0, 1] : \theta \in \{0, 1\}\},$$

with attractor

$$(19) \quad \Omega_{\text{dyadic}} := \bigcap_{t \geq 0} \bigcup_{\theta^0 \dots \theta^{t-1} \in \{0, 1\}^t} F_{\theta^{t-1}} \circ \dots \circ F_{\theta^0}([0, 1]).$$

This is a Cantor set with box dimension $\log(2)/\log(a^{-1})$.

In the typical case, when $\{T_{v_k v_{k+1}} : 1 \leq k \leq n+1\} \cap \Omega_{\text{dyadic}} = \emptyset$, we can associate, as before, to each internal vertex a depth

$$(20) \quad t_k := \max \{t \geq 1 : T_{v_k v_{k+1}} \in \cup_{\theta^0 \dots \theta^{t-1} \in \{0, 1\}^t} F_{\theta^{t-1}} \circ \dots \circ F_{\theta^0}([0, 1])\}.$$

In the present case we can recursively define the t_k approximation to the activity level, and the internal code as follows:

$$(21) \quad \begin{aligned} \mathbf{x}_{v_1}(\theta_{\text{in}}^{t-t_1} \dots \theta_{\text{in}}^{t-1}) &:= (1-a) \sum_{\tau=t-t_1}^{t-1} a^{t-\tau-1} \theta_{\text{in}}^\tau \\ \theta_{v_k v_{k+1}} &:= H \left(\sigma_{v_k v_{k+1}} \left(\mathbf{x}_{v_k}(\theta_{v_{k-1} v_k}^{t-t_k} \dots \theta_{v_{k-1} v_k}^{t-1}) - T_{v_{k-1} v_k} \right) \right) \\ \mathbf{x}_{v_{k+1}}(\theta_{v_k v_{k+1}}^{t-t_{k+1}} \dots \theta_{v_k v_{k+1}}^{t-1}) &:= (1-a) \sum_{\tau=t-t_{k+1}}^{t-1} a^{t-\tau-1} \theta_{v_k v_{k+1}}^\tau, \end{aligned}$$

for $1 \leq k < n$. According to this, the $(k+1)$ -th internal vertex, considered as an ET, works as the cellular automata $\Phi_k : \{0, 1\}^{\mathbb{N}} \rightarrow \{0, 1\}^{\mathbb{N}}$, such that

$$(22) \quad \Phi_k(\Theta)_t = \begin{cases} (1 - \sigma_{v_{k+1} v_{k+2}})/2 & \text{if } \mathbf{x}_{v_{k+1}}(\theta_{v_k v_{k+1}}^{t-t_{k+1}} \dots \theta_{v_k v_{k+1}}^{t-1}) < T_{v_{k+1} v_{k+2}} \\ (1 + \sigma_{v_{k+1} v_{k+2}})/2 & \text{otherwise.} \end{cases}$$

It follows that the output code of the whole RCh can be resolved with a delay $t_0 := \sum_{k=1}^n t_k$, by using the composition $\Phi := \Phi_n \circ \Phi_{n-1} \circ \dots \circ \Phi_1 : \{0, 1\}^{\mathbb{N}} \rightarrow \{0, 1\}^{\mathbb{N}}$.

The structure of each one of the cellular automata $\Phi_k : \{0, 1\}^{\mathbb{N}} \rightarrow \{0, 1\}^{\mathbb{N}}$ is such that if $\theta_{\text{in}}^{t-t_0} \dots \theta_{\text{in}}^{t-1}$ is a constant sequence, then

$$(23) \quad \Phi(\Theta)_t = \begin{cases} (1 - \sigma)/2 & \text{if } \theta_{\text{in}}^{t-t_0} \dots \theta_{\text{in}}^{t-1} = 00 \dots 0, \\ (1 + \sigma)/2 & \text{if } \theta_{\text{in}}^{t-t_0} \dots \theta_{\text{in}}^{t-1} = 11 \dots 1, \end{cases}$$

where $\sigma = \prod_{k=1}^{n-1} \sigma_{v_k v_{k+1}} \times \sigma_{v_n w}$ is the sign of the chain as defined above.

As for the ET, even if the dyadic attractor Ω_{dyadic} is not a Cantor set, the output code of the regulatory chain can be typically resolved for sequences of low input complexity. In this case the action can also be obtained as the composition $\Phi := \Phi_n \circ \Phi_{n-1} \circ \dots \circ \Phi_1 : \{0, 1\}^{\mathbb{N}} \rightarrow \{0, 1\}^{\mathbb{N}}$.

3.2.3. The general regulatory cascade.

As mentioned above a regulatory cascade is defined over a connected digraph with no cycles. The vertices of this digraph can be hierarchically organized, so that the input code for vertices in the k -th level are the output code of the vertices in the $(k-1)$ -th level. This way, following the same idea as in the analysis of the regulatory chain, we can resolve the output code of the cascade by using a composition of cellular automata associated to the vertices of the cascade.

The hierarchy of vertices is the following. On top we have the root vertices,

$$(24) \quad V_{\text{root}} := \{v \in V_{\text{mod}} : (u, v) \in A \Rightarrow u \in V_{\text{ext}}\},$$

which are the vertices in V_{mod} all of whose incoming arrows have tail in the set of external vertices. Let $V_0 = V_{\text{root}}$, $U_0 = V_0$, and for each $k \geq 1$ we define

$$(25) \quad \begin{aligned} V_k &:= \{v \in V_{\text{mod}} : (u, v) \in A \Rightarrow u \in U_{k-1} \cup V_{\text{ext}}\}, \\ U_k &:= U_{k-1} \cup V_k. \end{aligned}$$

We can see U_{k-1} as the union of all vertices up to the $(k-1)$ -th level. Then the k -th level, V_k , is composed by those vertices in V_{mod} all of whose incoming arrows have tail in levels lower than the k -th or in V_{ext} . Since the underlying digraph has no cycles or loops, then these levels are nonempty. Also, since the digraph V_{mod} is a finite set, there is a finite number of levels, all of them of finite size. Vertices of the last of these levels are called *leaf vertices*. This last level can also be defined by

$$(26) \quad V_{\text{leaf}} := \{v \in V_{\text{mod}} : (v, w) \in A \Rightarrow w \in V_{\text{ext}}\}.$$

The depth d of the regulatory cascade is the number of steps needed, starting from the root, to determine the leaf vertices, *i. e.* $V_d = V_{\text{leaf}}$.

Because of this hierarchical structure, and taking into account Equation (2), the activity level \mathbf{x}_v^t , for $v \in V_k$, is given by

$$(27) \quad \mathbf{x}_v^{t+1} := a\mathbf{x}_v^t + (1 - a) \left\{ \sum_{u \in I(v) \cap U_{k-1}} \kappa_{uv} H(\sigma_{uv}(\mathbf{x}_u^t - T_{uv})) + \sum_{u \in I(v) \cap V_{\text{ext}}} \kappa_{uv} \theta_{uv}^t \right\}.$$

If, on the other hand, we can resolve the internal codes $(\theta_{uv}^t : u \in I(v) \cap U_{k-1})$, then the previous equation reduces to

$$\mathbf{x}_v^{t+1} := a\mathbf{x}_v^t + (1-a) \left\{ \sum_{u \in I(v) \cap U_{k-1}} \kappa_{uv} \theta_{uv}^t + \sum_{u \in I(v) \cap V_{\text{ext}}} \kappa_{uv} \theta_{uv}^t \right\}.$$

Hence, all the internal vertices can be considered as ETs, and all what we discussed in paragraph 3.2.1 applies. Once again we have the alternative between the internally separable and the non-separable case.

1.- Internal separability for RC. Once again, the simplest case occurs when the IFS associated to each one of the internal vertices,

$$\mathcal{F}_v := \left\{ F_\theta(\mathbf{x}) = a\mathbf{x} + (1-a) \sum_{u \in I(v)} \kappa_{uv} \theta_{uv} : \theta \in \{0,1\}^{\#I(v)} \right\}$$

has a Cantor set Ω_v as attractor. In this simple case, with probability 1 none of the thresholds associated to internal arrows will lie inside its corresponding Cantor set, so that to the sequence of output codes from vertex v , $(\theta_{vv'}^t : (v, v') \in A)$ can be resolved with a finite delay t_v , by using a cellular automata $\Phi_v : (\{0,1\}^{\#I(v)})^{\mathbb{N}} \rightarrow (\{0,1\}^{\#O(v)})^{\mathbb{N}}$. Here $I(v)$ and $O(v)$ are respectively the input and output set of the vertex v , and the cellular automata Φ_v is defined in the same way as in Equation (16). The input sequence of the cellular automata associated to the internal vertex $v \in V_k$ is obtained from the input sequence of codes via the action of the cellular automata Φ_u associated to vertices in levels lower than k .

Example 3.2. Let us illustrate how operates a regulatory cascade in the internally separable case by considering the incoherent feedforward loop of Figure 3. This RC contains a positive regulatory chain $\rightarrow u \rightarrow v \rightarrow$, and an negative arrow from u to w . Let us fix $a = 1/5$, output threshold $T_{wv_{\text{out}}} = 1/2$, output sign $\sigma_{wv_{\text{out}}} = 1$, and coupling constants $\kappa_{uw} = 1 - \kappa_{vw} = 2/3$. In this way, the functioning of the vertex w considered as an ET could be deduced from that of Example 3.1.

Let $T_{uv} = 22/25$, $T_{uw} = 22/125$, and $T_{vw} = 1/2$. The IFS associated to these vertices is

$$\mathcal{F}_u = \mathcal{F}_v = \{F_0x = x/5, F_1x = x/5 + 4/5\},$$

which has a dyadic Cantor attractor Ω_v with box dimension $\log(2)/\log(5)$. The delays determined from the position of the thresholds with respect to the attractor are $t_u = 2$ and $t_v = 1$.

The internal code $(\theta_{uv}^t, \theta_{uw}^t)$ depends only on the input sequence Θ_{in} and it is given by

$$\begin{aligned} \theta_{uv}^t &= \begin{cases} 0 & \text{if } \theta_{\text{in}}^{t-2} \theta_{\text{in}}^{t-1} \in \{00, 01, 10\}, \\ 1 & \text{if } \theta_{\text{in}}^{t-2} \theta_{\text{in}}^{t-1} = 11. \end{cases} \\ \theta_{uw}^t &= \begin{cases} 1 & \text{if } \theta_{\text{in}}^{t-3} \theta_{\text{in}}^{t-2} \theta_{\text{in}}^{t-1} \in \{000, 001, 010\}, \\ 0 & \text{otherwise.} \end{cases} \end{aligned}$$

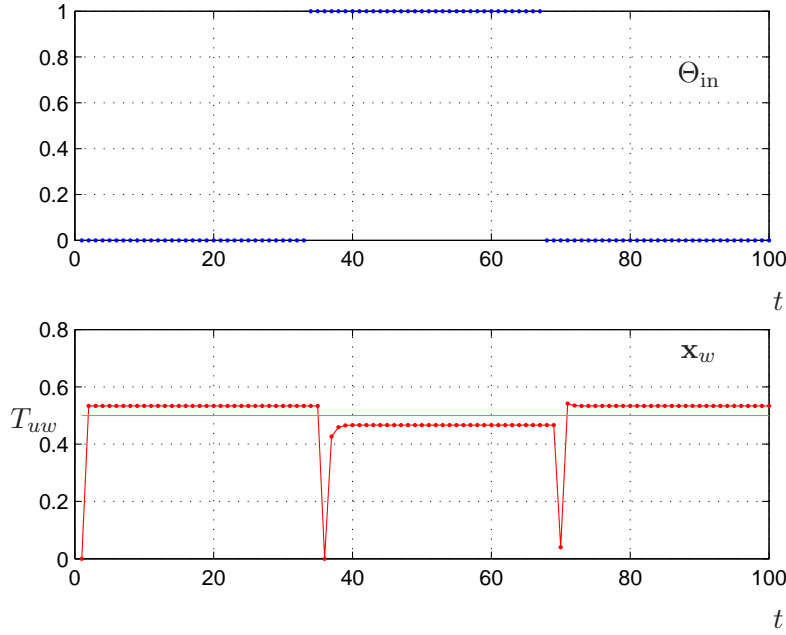


FIGURE 5. Behavior of the incoherent feedforward loop. On top, the input signal θ_u^t . Below, the state of the output vertex \mathbf{x}_w^t responsible of the output signal. The output signal changes each time \mathbf{x}_w^t crosses the output threshold indicated by a horizontal line in the figure.

For the $\text{RCh} \rightarrow u \rightarrow v \rightarrow$, the composition of $\Phi_v \circ \Phi_u$ allows to determine the internal code θ_{vw}^t directly from the input code Θ_{in} . We obtain the following:

$$\theta_{vw}^t = \begin{cases} 0 & \text{if } \theta_{\text{in}}^{t-3} \theta_{\text{in}}^{t-2} \in \{00, 01, 10\}, \\ 1 & \text{otherwise.} \end{cases}$$

Finally, considering the vertex w as an ET with two inputs we obtain an output code

$$\theta_{\text{out}}^t = \begin{cases} 1 & \text{if } \theta_{\text{in}}^{t-4} \theta_{\text{in}}^{t-3} \in \{00, 01, 10\}, \\ 0 & \text{if } \theta_{\text{in}}^{t-4} \theta_{\text{in}}^{t-3} = 11. \end{cases}$$

This feedforward loop operates as a cellular automata. The output code can be resolved with a delay $t_w = 4$.

2.- The general case. The output code cannot be determined solely from the input code when at least one of the attractors Ω_v is not a Cantor set, or when one of the thresholds $T_{vv'}$ is contained in its corresponding attractor Ω_v . In those cases, for each depth $\tau \in \mathbb{N}$ there are sequences of input codes such that the output code cannot be resolved in finite time. The comment made in Paragraph 3.2.1 concerning sequences of input codes with low temporal

complexity applies once again. In that case we can typically resolve the output code in finite time.

Remark 3.2 (Comments on decrease of complexity). Each time we can resolve the output code in finite time, whether we are in the internally separable case or because the low input complexity holds, the RC operates as a cellular automata $\Phi : (\{0, 1\}^{\#A_{\text{in}}})^{\mathbb{N}} \rightarrow (\{0, 1\}^{\#A_{\text{out}}})^{\mathbb{N}}$ such that

$$\Phi(\Theta_{\text{in}})_t = \phi(\theta_{\text{in}}^{t-t_0} \theta_{\text{in}}^{t-t_0+1} \dots \theta_{\text{in}}^{t-1}).$$

The symbolic complexity of the output code is the counting function $C_{\Theta_{\text{out}}} : \mathbb{N} \rightarrow \mathbb{N}$ such that

$$(28) \quad C_{\Theta_{\text{out}}}(t) := \# \{ \theta_{\text{out}}^{\tau} \dots \theta_{\text{in}}^{\tau+t} : \tau \in \mathbb{N} \},$$

i. e., for each $t \in \mathbb{N}$, $C_{\Theta_{\text{out}}}(t)$ counts all different sequences of output codes of length t . In the present case, since the output code can be resolved with a delay t_0 , we clearly have

$$(29) \quad C_{\Theta_{\text{out}}}(t + t_0) \leq C_{\Theta_{\text{in}}}(t) + \left(2^{\#W}\right)^{t_0}.$$

In the case of an exponentially increasing complexity the previous inequality ensures the non-increase of the entropy [14].

4. FORCED CIRCUITS

Forced circuits (FC) are modules in a regulatory network such that the underlying graph $(V_{\text{mod}}, A_{\text{mod}})$ is a circuit.

Examples of forced circuits are the (open) Negative Auto Regulator (NAR), the Positive Auto Regulator (PAR) and the network motifs with double-positive (or double-negative)-feedback loop [3].

In this section we focus on special cases of FC in order to show the strategy of analysis as well as the reach possibilities of dynamical behaviors displayed by such modules. Not surprisingly, each one may show different behaviors according to the inputs. In particular, in most cases the dynamical behavior of the module (open system) is different from that of the same system when isolated.

4.1. The self-regulations.

Self-regulation occurs when a transcription factor acts as an inhibitor (self-inhibitor or NAR) or an enhancer (self-activation or PAR) of the transcription of its own gene. Self-regulation is a very common situation, for instance it is involved in over 40% of known *E. coli* transcription factors [22].

For a self-regulator subjected to a single input arrow as indicated in Figure 6, thanks to the normalization condition $\kappa_{vv} + \kappa_{uv} = 1$, the Equations (1) and (2) read:

$$(30) \quad \mathbf{x}_v^{t+1} = a\mathbf{x}_v^t + (1-a) \left[H(\sigma_{vv}(\mathbf{x}_v^t - T_{vv})) + \kappa_{uv}(\theta_{uv}^t - H(\sigma_{vv}(\mathbf{x}_v^t - T_{vv}))) \right],$$

From (1), we see that for $\kappa_{uv} = 0$ one recovers the isolated self-regulation.

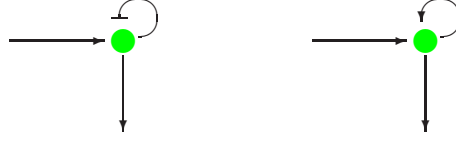


FIGURE 6. The open self-regulation, left: $\sigma_{vv} = -1$ for a self-inhibition; right: $\sigma_{vv} = +1$ for a self-activation.

Otherwise, for each given σ_{vv} there are two extra parameters, the input intensity κ_{uv} and the input signal sequence $\Theta_{\text{in}} := (\theta_{uv}^t)_{t \in \mathbb{N}}$ (also called “exogene variable”). As usual we write $H(\sigma_{vv}(\mathbf{x}_v - T_{vv})) = \theta_{vv}$ and then we merge internal and external codes in a unique symbol: $\theta^t = \theta_{vv}^t \theta_{uv}^t$ (*internal on the left, input on the right*).

As a first approximation, an easy way to visualize the different dynamics when changing the parameters and/or the input signal sequence is to show a diagram with the possible transitions among the θ s at each time step (see Figure 9 (B)), known as dynamical graphs [23, 9, 7]. In particular, it allows to locate forbidden paths in phase space and therefore localize the most robust bifurcations. Because residence times in each loop are not specified in this diagram, dynamical graphs carry only part of the dynamical information.

We shall describe in the following the case of the self-inhibition in detail and then, for conciseness, we only sketch the case of the self-activation.

4.1.1. The open self-inhibition.

The dynamics of an isolated self-inhibitor, NAR, consists only of oscillations [6]. In fact, whenever $0 < T_{vv} < 1$, this system is conjugated to a rotation on a circle with a rotation number $\nu(a, T)$ depending on the parameters [5, 6].

Figure 7 illustrates the three possible cases of the dynamics for the open self-inhibitor, shown Figure 6, when varying the input intensity. Accordingly, the parameter subspace $\{(T_{vv}, a, \kappa_{uv}) : T_{vv} \in (0, 1), a \in [0, 1) \text{ and } \kappa_{uv} \in [0, 1]\}$ can be divided into three input intensity regions, corresponding to different dynamical behaviors. **Region I:** if $\kappa_{uv} < T_{vv}$, **Region II:** if $T_{vv} < \kappa_{uv} < 1 - T_{vv}$ and **Region III:** if $\kappa_{uv} > T_{vv}$.

Remark 4.1. Up to a change of $(\theta_{vv}, \theta_{uv})$ in $(1 - \theta_{vv}, 1 - \theta_{uv})$ in the dynamical graphs, it is enough to consider the cases where $T_{vv} < 1 - T_{vv}$.

Figure 8 displays the response of the self-inhibitor circuit to an input in Region I and Region III. The input θ_u^t is set to 0 for $0 \leq t < 20$, then equal to 1 for $20 \leq t \leq 40$ and then again to 0 for $40 < t < 50$. Therefore, the dynamics is governed by the branches f_{00} and f_{10} during the first and the last period and by f_{01} and f_{11} during the intermediate time. It is clear from Figure 7 that the response is very different in case (A) of small input intensity and (C) of

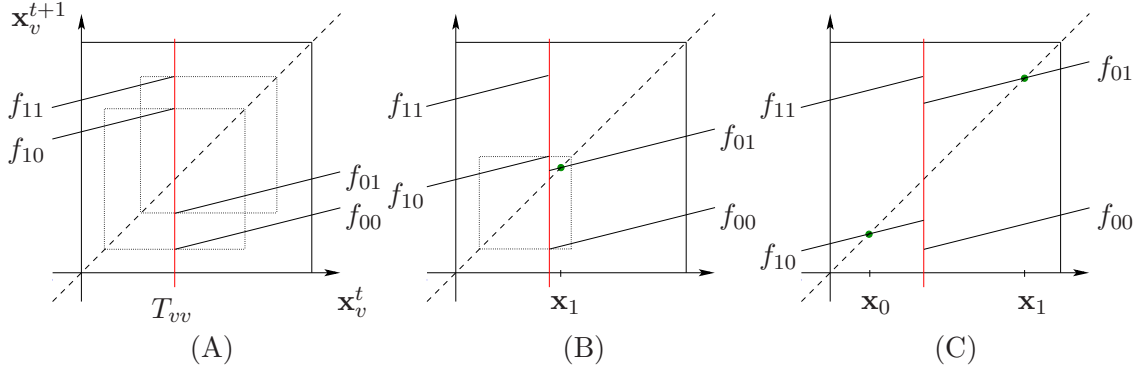


FIGURE 7. **The open self-inhibition:** graphs of the IFS $F_{\theta_{uv}}(\mathbf{x}_v) = a\mathbf{x}_v + (1 - a)[H(T_{vv} - \mathbf{x}_v) + \kappa_{uv}(\theta_{uv} - H(T_{vv} - \mathbf{x}_v))]$ For, (A) Region I, small input intensity κ_{uv} , (B) Region II, intermediate input intensity and (C) Region III, high input intensity. Possible fixed points are given by the intersection of the graph with the diagonal. The notation $f_{ij}, i, j = 0, 1$ stands for the branch of F_i when $H(T_{vv} - \mathbf{x}_v) = i$ and $\theta_{uv} = j$.

high input intensity. In the first case there are no available fixed points and the system runs in pure oscillations and only the amplitude and the frequency distinguish the lower from the upper level of the input. In the last case the system contracts to the lower fixed point (see f_{10}) for lower level activation and to the upper fixed point (see f_{01}) for high level input. It is clear in this example that the input intensity may change the dynamical behavior of a module from oscillatory to bistable.

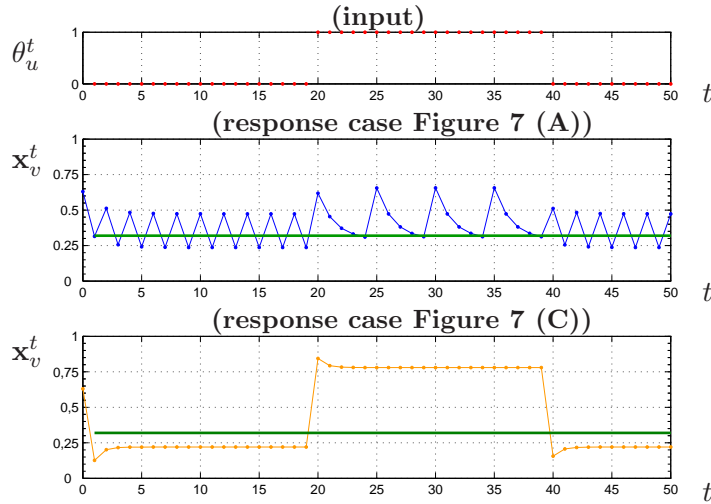


FIGURE 8. **The open self-inhibition:** The typical response \mathbf{x}_v^t to the input \mathbf{x}_u^t : (A) in Region I, small input intensity κ_{uv} , (C) in Region III, high input intensity. The horizontal green line indicates the output threshold.

In Figure 9, these three regions of parameters are subdivided in smaller subregions corresponding to different dynamical graphs and therefore to possibly different dynamical regimes that we describe in the following.

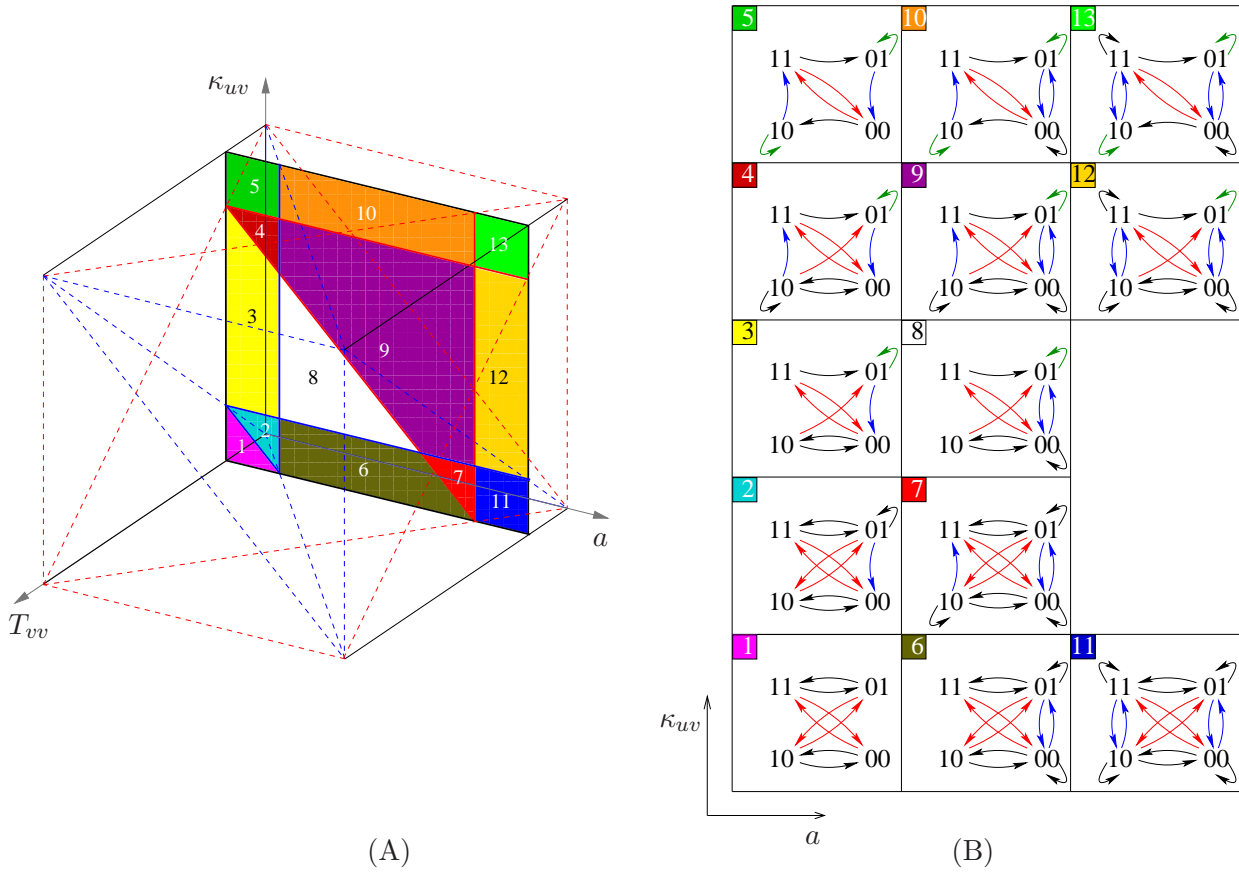


FIGURE 9. For the open self-inhibition, (A) Parameter space. It is made of 13 subregions. Different colors, depicted for a given T_{vv} , show how the κ_{uv} parameter can affect the dynamics. (B) Corresponding dynamical graphs of possible transitions. The code denotes $\theta_{vv}\theta_{uv}$. Colours are in correspondence with the plane in (A). **Region I:** includes 1, 2, 6, 7, 11, **region II:** 3, 4, 8, 9, 12 and **region III:** 5, 10, 13.

1.- Region I. For $\kappa_{uv} < T_{vv}$, corresponding to Figure 7 (A), the dynamics is the same as for the isolated self-inhibitor, *i. e.*, \mathbf{x}_v oscillates whatever the input sequence can be, but with

an amplitude and a frequency that depend on the input $(\theta_{uv}^t)_{t \in \mathbb{N}}$. This is because in this case the corresponding maps have no fixed points.

If a is small enough (subregion 1), the system will change code at each time and the next code is completely defined by the external input at that time, Figure 9 (B). In particular, for a constant input sequence the coding of the oscillating orbits $(\mathbf{x}_v^t)_{t \in \mathbb{N}}$ does not depend on the initial condition \mathbf{x}_v^0 .

For higher a values (subregions 2, 6, 7 and 11), the input sequence $(\theta_{uv}^t)_{t \in \mathbb{N}}$ can non-trivially affect the dynamics of x_v . This corresponds to the occurrence of the loops in the dynamical graph, allowing the orbit to lie inside a given atom of the symbolic partition more than one time step depending of the input sequence. The reason is clear: as a increases the image of the branches (see Figure 7 (A)) may intersect the two sides of the discontinuity.

Remark 4.2 (The general case: local fixed points and absorbing intervals). One can consider the more general case of any number of inputs. Again the existence of local fixed points for the IFS $F_{\theta_{uv}}$ depends on the internal and external parameter values. Let P be the number of local fixed points for $F_{\theta_{uv}}$. Let $S_r(v)$ be any subset (possibly empty) of $I(v)$ such that $\sum_{u \in S_r(v)} \kappa_{uv} > T_{vv}$ and let R be the number of such subsets. Let $S_l(v)$ be any subset (possibly empty) of $I(v) \cup \{v\}$ containing $\{v\}$ such that $\sum_{u \in S_l(v)} \kappa_{uv} \leq T_{vv}$ and L be the number of such subsets. It is not difficult to see the relation: $P = L + R$. Consequently $0 \leq P \leq 2^{\#I(v)}$.

Similarly, let A be the number of local absorbing intervals $\subset (0, 1)$ and let $S_c(v)$ be any subset (possibly empty) of $I(v)$ and $\bar{S}_c(v) = S_c(v) \cup \{v\}$ such that $\sum_{v \in S_c(v)} \kappa_{uv} \leq T_{vv} < \sum_{u \in \bar{S}_c(v)} \kappa_{uv}$, and C be the number of such subsets. Then $A = C$. Consequently $0 \leq A \leq 2^{\#I(v)}$.

Finally one can check that $P + A = L + R + C = 2^{\#I(v)}$. The two extrem cases are $P = 0 \Leftrightarrow A = 2^{\#I(v)}$ if and only if $1 - \kappa_{vv} \leq T_{vv} < \kappa_{vv}$, and $P = 2^{\#I(v)} \Leftrightarrow A = 0$ if and only if $\kappa_{vv} \leq T_{vv} < \min_{u \in I(v)} \{\kappa_{uv}\}$ or $K_{vv} + \max_{u \in I(v)} \{\kappa_{uv}\} \leq T_{vv} < 1 - \kappa_{vv}$.

Externally induced switches from (projected) fixed point converging regimes to (projected) periodic orbit converging regimes, and vice versa, give fairly simple dynamics. It results in the concatenation of pieces of (transient) orbits from either regimes. Switches between periodic orbit converging regimes may however be quite complicated as we see it next.

2.- Region III. For the opposite case, i. e. for $\kappa_{uv} > 1 - T_{vv}$ corresponding to Figure 7 (C), we notice the occurrence of two fixed points. The first, denoted \mathbf{x}_0 , corresponds to the branch f_{10} and therefore an orbit will come close to it by the repeated injection of the corresponding input $\theta_{uv} = 0$. The second one, \mathbf{x}_1 , corresponds to the branch f_{01} and an orbit will come close to it by the repeated injection of the corresponding input $\theta_{uv} = 1$. Therefore, in this case, the internal code θ_{vv} is a delayed slave of the input code θ_{uv} provided the forcing is permanent enough.

In this sense the NAR behaves in this region of parameters as the RC described in the previous section.

In particular, if $(\theta_{uv}^t)_{t \in \mathbb{N}}$ is constant (t -independent), then there exists a $t^0 \geq 0$ such that $\theta_{vv}^t = 1 - \theta_{uv}^t \forall t \geq t^0$, so that the system can be easily driven in one of the two different states as if it was bistable.

Notice that in the dynamical graphs of Figure 9 (B), for the corresponding subregions 5, 10 and 11, whatever the input sequence is, the loops that do not correspond to codes 10 or 01 cannot consecutively be taken an infinite number of times and the (finite) number of residence steps will depend on the input sequence after some delay.

If the input sequence $(\theta_{uv}^t)_{t \in \mathbb{N}}$ is not constant, then the internal code $(\theta_{vv}^t)_{t \in \mathbb{N}}$ will depend on the initial condition \mathbf{x}_v^0 . In this case, depending of the parameters, the proper mathematical study of the internal code sequences that correspond to a given input sequence is still an open problem.

The converse statement can however be formulated and is also of practical interest. Namely, being given an observed internal sequence, what are the possible inputs and internal parameter values of the self-inhibition that realize that observed sequence?

We now present an example showing that the use of *admissibility conditions* as in [6], implemented in a numerical algorithm, allows to produce such sequences for each particular occurrence.

Example 4.1. Let us illustrate the identification procedure in the case of a periodic orbit of an open self-inhibition with the observed internal sequence $(01001)^\infty$ of period 5.

First, we identify within Figure 9 (B) the candidate dynamical graphs to realize the observed sequence, and then the families of input sequence provided by those graphs. In our example the candidate input sequences $(\theta_{uv}^t)_{t \in \mathbb{Z}}$ are the families (with $\omega \in \{0, 1\}$):

- $(\omega\omega 1\omega\omega)^\infty$ for 2,
- $(0\omega 10\omega)^\infty$ for 3 and 4,
- $(01101)^\infty$ for 5,
- $(\omega\omega\omega\omega\omega)^\infty$ for 6, 7 and 11,
- $(0\omega\omega 0\omega)^\infty$ for 8, 9 and 12,
- $(01\omega 01)^\infty$ for 10 and 13.

Notice that no transitions in the graph 1 can produce the observed internal code.

Then we choose one input sequence among the more robusts. Those are the one appearing in the greatest number of dynamical graphs. This criterion makes more likely the set of parameter values that realize the observed internal code for that candidate input code to be broad in the parameter space. This way we select the candidate sequence $(01101)^\infty$ common to all transition graphs except 1, and for comparison we also consider $(00111)^\infty$ that is only possible for 2, 6, 7 and 11.

Thirdly, we explicit the admissibility condition with the internal and the candidate input codes, and solve it. The admissibility condition writes:

$$(31) \quad \sup_{t \in \mathbb{Z}: (\theta_{uu}^t, \theta_{uv}^t) \in \{1\} \times \{0, 1\}} \mathbf{x}^t \leq T_{uu} \lesssim \inf_{t \in \mathbb{Z}: (\theta_{uu}^t, \theta_{uv}^t) \in \{0\} \times \{0, 1\}} \mathbf{x}^t,$$

with for a fixed $(a, \kappa_{uv}) \in [0, 1) \times [0, 1]$,
(32)

$$\{\mathbf{x}^t : t \in \mathbb{Z}\} = \left\{ 1 - \frac{1-a}{1-a^5} \left[(1-\kappa_{uv}) \sum_{k \in I_s} a^{(n+k) \bmod 5} + \kappa_{uv} \sum_{k \in E} a^{(p+k) \bmod 5} \right] : (n, p) \in \llbracket 0, 4 \rrbracket^2 \right\}.$$

In the last expression $I_s = \{k \in \llbracket 0, 4 \rrbracket \mid \sigma^{-1}(\theta_{uu}) = 0 \text{ and } \sigma^{-k-1}(\theta_{uu}) = 0 \text{ if } s = 0 \text{ and } \sigma^{-k-1}(\theta_{uu}) = 1 \text{ if } s = 1\}$, and $E = \{k \in \llbracket 0, 4 \rrbracket \mid \sigma^{-1}(\theta_{uv}) = 0 \text{ and } \sigma^{-k-1}(\theta_{uv}) = 0\}$, σ being the left shift map in $\{0, 1\}^{\mathbb{Z}}$. We have explicitly in our case $I_0 = \{1, 2, 4\}$, $I_1 = \{0, 3\}$, and $E = \{2, 4\}$.

The results are shown Figure 10 with the plot of all the (a, T_{vv}) values admissibles for a fixed value of κ_{uv} . As expected from the analysis of the transition graphs, the domain for $(00111)^\infty$ appears smaller than the domain for $(01101)^\infty$ when varying the κ_{uv} parameter.

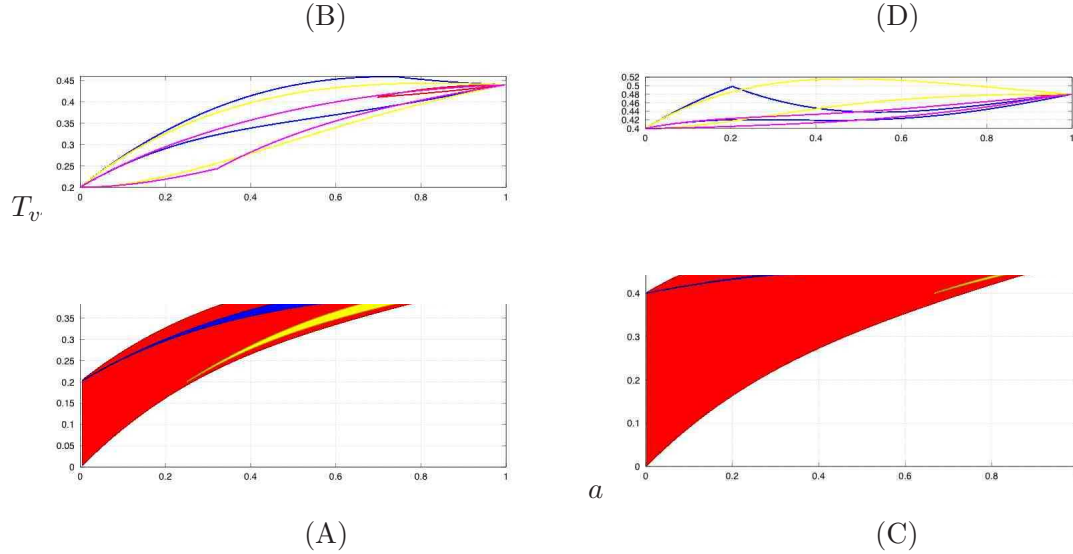


FIGURE 10. (a, T) subdomains of admissibility for the periodic input $(01101)^\infty$ with $\kappa_{uv} = 0.2$ (A) and $\kappa_{uv} = 0.4$ (B), and for the periodic input $(00111)^\infty$ with $\kappa_{uv} = 0.2$ (C) and $\kappa_{uv} = 0.4$ (D). For (A) and (C) the admissible values are within the colored areas while for (B) and (D) the admissible values are in between the colored boundaries. The area and boundary colors are in correspondance.

One can see the overlap of the domains for a given value of κ_{uv} (Compare (A) and (B) for instance), meaning that the same observed internal sequence can be observed for the same parameter values for different input sequences. It illustrates the robustness to that parameter.

Also, depending on the input sequence there may have a dependence to the initial condition. This is illustrated on Figure 10 where each color corresponds to an attracting periodic orbit with its basin of attraction. Furthermore, although all the attracting periodic orbits may have the same period, they differ in particular by their amplitude. Another way to present

it is that in practice different realizations may look similar (frequency) but differ (in the state at a given time, in amplitude) depending on the initial condition.

Finally, notice the qualitative relation between the domains of Figure 10 and those of Figure 9 (A). The sequence $(01001)^\infty$ is indeed for the input $(01101)^\infty$ out of the tetrahedron $\boxed{1}$ as indicated by the derivative of the upper bound of the red domain at $a = 0$ Figure 10 (A). Also The sequence $(01001)^\infty$ is indeed for the input $(00111)^\infty$ out of the tetrahedron $\boxed{8}$.

Remark 4.3. System identification is closely related to the control issue, as if we can find out an input and parameter values that realize a given behavior of the module, then that input, with the appropriate parameter values, can also be used to control the module to a desired behavior. Furthermore the robustness to small additional perturbations has been illustrated on Figure 10.

3.- Region II. We first treat the case $1 - \kappa_{uv} < \kappa_{uv}$.

If $T_{vv} \leq \kappa_{uv} < 1 - T_{vv}$, corresponding to Figure 7 (B), the dynamics shares the characteristics of both previous systems. This is because in this parameter region only the branch f_{01} (matching the input $\theta_{uv} = 1$) induces a fixed point, while on the branch f_{00} the system will oscillate in any case. That is to say: if $\theta_{uv}^t = 1 \ \forall t \in \mathbb{N}$, then any orbit converges asymptotically to \mathbf{x}_1 , if $\theta_{uv}^t = 0 \ \forall t \in \mathbb{N}$, then the dynamics is as for the pure self-inhibition, up to a change of variable that depends on κ_{uv} (the same as for region I).

The region II contains three subregions denoted 3, 4, 8, 9 and 12 in Figure 9. Again, depending on the subregion, some transitions, in presence of a suitable input, are possible or not. As in the previous case, and for the same reason, only the loop corresponding to 01 in the dynamical graph may be taken an infinite number of consecutive time steps. Again, the (finite) number of residence steps in the remainder codes will depend on the input sequence after some delay.

In case that $\kappa_{uv} < 1 - \kappa_{uv}$, due to the symmetry $\kappa_{uv} \longleftrightarrow 1 - \kappa_{uv}$ we shall have in Region II a steady low level state $\mathbf{x}_0 < T_{vv}$ corresponding to the input $\theta_{uv}^t = 0$ and high level oscillation corresponding to the input $\theta_{uv}^t = 1$.

Finally, we see that depending on the parameter values of the circuit and on the different inputs the circuit may either oscillations, exhibit a low level or a high level steady state, or even be bistable.

This analysis shows that the range of external signals can have a significant influence on the expression dynamics of a self-inhibited gene. Depending on the input signal and/or the self-regulation parameters, very different dynamical regimes can exist and satisfy different functional 'demands' of the whole regulatory network through the subsequent interactions the gene is involved in.

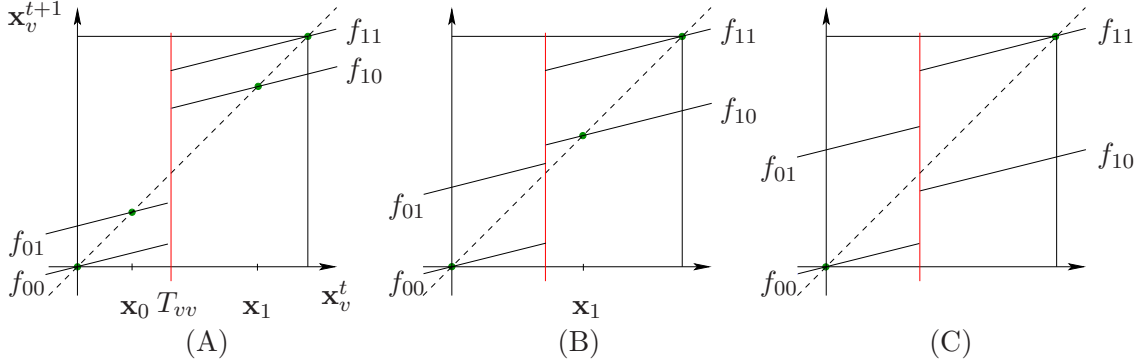


FIGURE 11. **The open self-activation.** Graphs of the IFS $F_{\theta_{uv}}(\mathbf{x}_v) = a\mathbf{x}_v + (1 - a)[H(\mathbf{x}_v - T_{vv}) + \kappa_{uv}(\theta_{uv} - H(\mathbf{x}_v - T_{vv}))]$. For (A) Region I, small input intensity, (B) Region II, intermediate input intensity and (C) Region III, high input intensity. Possible fixed points are given by the intersection of the graph with the diagonal. The notation $f_{ij}, i, j = 0, 1$ stands for the branch of $F_{\theta_{uv}}$ when $H(\mathbf{x}_v - T_{vv}) = i$ and $\theta_{uv} = j$.

4.1.2. The open self-activation.

We now proceed with the positive self-regulation (PAR). An isolated PAR is a bistable system apart from the (non functional) case where $T_{vv} \notin [0, 1]$ [6].

Figure 11 illustrates the three possible cases of the dynamics for the corresponding open system, shown Figure 6, when varying the input intensity. Accordingly, as in the case of the self-inhibition, it follows that the parameter subspace $\{(T_{vv}, a, \kappa_{uv}) : T_{vv} \in (0, 1), a \in [0, 1) \text{ and } \kappa_{uv} \in [0, 1]\}$ can be divided into three input intensity regions corresponding to different dynamical characteristics. The corresponding parameter domains are as for the NAR: **region I**: if $\kappa_{uv} < T_{vv}$, **region II**: if $T_{vv} < \kappa_{uv} < 1 - T_{vv}$ and **region III**: if $\kappa_{uv} > T_{vv}$.

Depending of the input intensity, some or all of the possible fixed points are present: 0 and \mathbf{x}_0 corresponding to the input $\theta_{uv} = 0$ (0 is present for all values of the input intensity) and (\mathbf{x}_1 and 1 corresponding the input, $\theta_{uv} = 1$ (see Figure 11). Note that 1 is present for all values of the input intensity.

Remark 4.4. We will consider only the cases were $T_{vv} < 1 - T_{vv}$ for the same reason than for the open self-inhibition.

1.- Region I. For $\kappa_{uv} < T_{vv}$, corresponding to Figure 11 (A), there exists two absorbing regions, $(0, \mathbf{x}_1)$ and $(\mathbf{x}_0, 1)$, for the orbits $(\mathbf{x}_v^t)_{t \in \mathbb{N}}$ on each side of the threshold T_{vv} whose size is fixed by the input intensity κ_{uv} . (Notice that if $\kappa_{uv} = 0$ then the dynamics is that of the isolated self-activation.)

Therefore, for a constant input sequence the dynamics is bistable and an orbit \mathbf{x}_v^t converges to either 0 or \mathbf{x}_0 , depending on the initial condition, if $\theta_{uv}^t = 0 \forall t$, or to either \mathbf{x}_1 or 1 if $\theta_{uv}^t = 1 \forall t$.

If θ_{uv}^t is not constant, then the dynamics of \mathbf{x}_v^t is driven by the input sequence, with possible oscillations within one of the two absorbing intervals $(0, \mathbf{x}_1)$ and $(\mathbf{x}_0, 1)$.

2.- Region III. For $\kappa_{uv} \geq 1 - T_{vv}$, corresponding to Figure 11 (C), whatever the value of a , if the input sequence is constant then the dynamics has one fixed point, at 0 if $\theta_{uv} = 0$ and at 1 if $\theta_{uv} = 1$.

In this input intensity region the open self-inhibition is a slave to the input sequence. It exhibits, however, a faster convergence to either fixed point if the input intensity κ_{uv} is close to T_{vv} , [3].

As for the self-inhibition in the same range of parameters, if the input sequence $(\theta_{uv}^t)_{t \in \mathbb{N}}$ is not constant, then the internal code $(\theta_{vv}^t)_{t \in \mathbb{N}}$ will depend on the initial condition \mathbf{x}_v^0 and again, using the *admissibility conditions* as in [6], it is possible to produce such sequences in each particular (see Example 4.1).

3.- Region II. We start with the case $1 - \kappa_{uv} < \kappa_{uv}$.

If $T_{vv} \leq \kappa_{uv} < 1 - T_{vv}$ (see Figure 11 (B)), depending on the input sequence $(\theta_{uv}^t)_{t \in \mathbb{N}}$, the dynamics can be either monostable, with attracting fixed point 1 if $\theta_{uv}^t = 1 \forall t$, bistable with two possible attracting fixed points 0 and \mathbf{x}_0 depending on initial conditions if $\theta_{uv}^t = 0 \forall t$, or showing more complicated (oscillating) dynamics if θ_{uv}^t is not constant.

As for the open self-inhibition circuit if $\kappa_{uv} < 1 - \kappa_{uv}$, due to the symmetry $\kappa_{uv} \longleftrightarrow 1 - \kappa_{uv}$ the dynamics in Region II can be either monostable, with attracting fixed point 0 if $\theta_{uv}^t = 0 \forall t$, or bistable with two possible attracting fixed points 1 and \mathbf{x}_1 depending on initial conditions if $\theta_{uv}^t = 1 \forall t$.

Finally we see that, depending on the parameter values of the circuit and on the different inputs, the circuit may either oscillate, or be bistable for both inputs, or to show a low level or a high level steady state and bistability.

This classification of the different dynamical regimes may be refined exactly in the same way as for the open self-inhibitor. It is clear from the analysis made for the NAR that crossing in the parameter space the same limits as for the self-inhibitor will cause robust bifurcations, leading to changes in the corresponding dynamical graph.

Finally, as for the self-inhibition, this analysis shows that the range of external signals can have a significant influence on the expression dynamics of a self-activated gene. Depending on the input signal and/or the self-regulation parameters very different dynamical regimes can exist.

4.2. The open negative 2-circuit.

The dynamics of the negative 2-circuit is studied in detail in [6]. It has a very reach dynamics including periodic and quasi-periodic attractors that may coexist for certain parameter values and there are no fixed points. These attractors organize the dynamics in the phase space. We shall describe the main features of the dynamics of the open negative 2-circuit shown in Figure 12, as compared with the autonomous system.

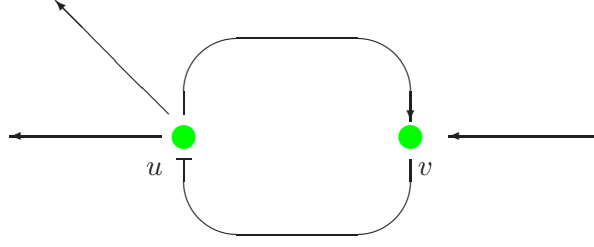


FIGURE 12. The open negative 2-circuit.

According to the last comment in section 2.2, it is important to understand first the cases where the forcing sequences are constant, $\theta_{\text{in}}^t = 0$ or $\theta_{\text{in}}^t = 1$ for all t . For $\theta_{\text{in}}^t = 0$ and 1, consider the two maps F_θ as in (6) and denote \mathbf{x}_θ their fixed points different from 0 and 1.

There are two completely different cases for that system.

First, *the oscillatory induced regime* that works as for the autonomous negative circuit: if $T_{vv} < \mathbf{x}_0$ and for 0 as input, any trajectory of the \mathbf{x}_v component of F_0 will end up after a finite number of time steps inside the invariant interval $[0, \mathbf{x}_0)$ and from there, up to an affine change of variables, the dynamics of F_0 behaves as the negative autonomous 2-circuit studied in [6]: i. e. it oscillates. The symmetric situation occurs for $\mathbf{x}_1 < T_{vv}$ and 1 as input. After a finite number of steps the dynamics of the \mathbf{x}_v component of F_1 oscillates inside the interval $(\mathbf{x}_1, 1]$. In short, the two variables \mathbf{x}_u and \mathbf{x}_v oscillate out of phase (by $\pi/2$). In case of 0 forcing they oscillate at a low level and in case of 1 as input at a high level. This situation occurs after some transient time if the initial condition of \mathbf{x}_v happen to be outside the corresponding invariant interval.

Second, *the fixed induced regime* which is different from the autonomous case: if $T_{vv} > \mathbf{x}_0$ and for 0 as input, any trajectory will be attracted by the unique fixed point of F_0 . This fixed point is $(1, \mathbf{x}_0)$. The reason is that, after a finite time we get $\mathbf{x}_v^t < T_{vv}$ and from then the signal θ_{vu}^t sent to node u is always 1 (since this interaction is an inhibition). As consequences, $\mathbf{x}_u \rightarrow 1$ and the signal θ_{uv}^t sent to node v is then always 1 (since now this interaction is an activation). Therefore, also $\mathbf{x}_v \rightarrow \mathbf{x}_0$. Finally, in this case, for a 0 as input, the circuit ends up in $\mathbf{x}_u = 1, \mathbf{x}_v = \mathbf{x}_0$. The case $\mathbf{x}_1 > T_{vv}$ and 1 as input is solved in the same way, and the circuit ends up in $\mathbf{x}_u = 0, \mathbf{x}_v = \mathbf{x}_1$.

Notice that in the fixed induced case, contrarily to the autonomous circuit, it is not the initial conditions that determines the final destination of the system but the external input.

Now, by a convenient choice of the external versus internal intensity it is possible to set $\mathbf{x}_0 < \mathbf{x}_1$ or $\mathbf{x}_0 > \mathbf{x}_1$. Therefore there are four possible open negative 2-circuits: (1) the bi-oscillating circuit that oscillates at small amplitude for a low level input and at a high amplitude for a high level input; (2) the oscillating-fixed circuit that oscillates at low amplitude for low level input and converges to $\mathbf{x}_u = 0, \mathbf{x}_v = \mathbf{x}_1$ for high level input; (3) the fixed-oscillating circuit converging to $\mathbf{x}_u = 1, \mathbf{x}_v = \mathbf{x}_0$ for low level input and oscillating for

high level input and (4) the bistable circuit that converges to $\mathbf{x}_u = 1$, $\mathbf{x}_v = \mathbf{x}_0$ or to $\mathbf{x}_u = 0$, $\mathbf{x}_v = \mathbf{x}_1$ according to a low or high input level.

Finally, for a more general (time variable) input this open circuit may work in different manners and, by appropriately tuning the forcing it is possible to switch the circuit from one regime to another.

By the same arguments, the open negative 2-circuit with reversed sign of interactions works in the same manner.

4.3. The open positive 2-circuit.

The same type of argument shows that for a positive 2-circuit and a constant external forcing, in one case it is bistable as is the autonomous system [6], but becomes monostable in the opposite case. Therefore, it is also possible to build bistable–bistable, bistable–monostable, monostable–bistable and monostable–monostable circuits working in the pointed regimes for low–high input levels.

Again it is clear in this case that an open positive circuit may operate in a regime different from the autonomous counterpart. In particular, an oscillatory input may drive the positive circuit in oscillations.

Notice that in [1] the same discrete–time piecewise–affine model have been numerically studied to account for the dynamics of a p53–Mdm2 genetic regulatory network made of an open positive and an open negative 2-circuit in interaction, with one inward regulation acting on each of the two circuits. In our notation, node u stands for p53 and node v for Mdm2.

The analysis above extend to the case of open n -circuits, in the same way as for the corresponding autonomous circuits [6].

5. EXAMPLE OF MIXED TYPE

In the more general case when a module owns one or more circuits inside a regulatory cascade it is in principle possible to combine our results and describe all its possible dynamical behaviors. For large networks this method will soon end up in the study of the network as a all and therefore it is of any help. However for simple networks the splitting of the all network in elementary RC and FC modules may help the study of their dynamics. As an example let us consider the incoherent type 1 feedforward loop (I1–FFL) [3], depicted in Figure 13. We first determine the possible dynamical regimes for the open self–inhibitor present at the level of GalS. Since there are two external inputs for this circuit (CRP and galactose) its dynamics displays four branches, corresponding to the possible combinations of the two inputs.

Therefore we can organize this information in a 2×2 table where say, arrows correspond to $\theta_{CRP, GalS} = 0$ or 1 and columns to $\theta_{galactose} = 0$ or 1 (notice that, because galactose repress GalS, according to our notation, $\theta_{galactose} = 0$ stands for high galactose level and $\theta_{galactose} = 1$ for low level). Now by looking for intensities of the interactions and thresholds, each entry of

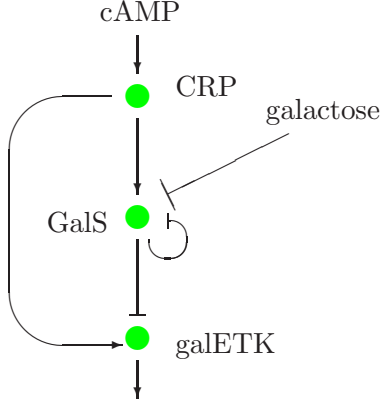


FIGURE 13. Incoherent feedforward loop of the type 1 from [3, pag. 454].

this table can be filled on the basis of the 3 possibilities described in 4.1.1: steady low level, steady high level or oscillation. In each case this information immediately fixes $\theta_{GalS,galETK}^{t+\tau_2}$ where τ_2 is the delay due to the interaction $GalS, galETK$ as described in 3.2.3. Notice also that $\theta_{CRP,GalS}^t$ is just equal to the input signal $\theta_{cAMP}^{t-\tau_1}$ after the delay τ_1 due to the node CRP .

Of course the delays τ_1 and τ_2 are only important during a transient time after one of the external signals eventually changed (as it is the case for a pulse input). If not, time translation invariance of the inputs simplify the analysis.

It is then sufficient to incorporate this information in the description of the dynamics of the RC made in 3.2.3. As a consequence this module can end up with, either an oscillatory regime for the final gene operon $galETK$ corresponding to an input corresponding to an “oscillation” entry of the table, or in a “steady state” (low or high level) for an input with this entry.

We emphasize that this module may operate in very different regimes either by a change of parameters (due for instance to a mutation) or by some modulation of the input signals, or both.

6. FINAL COMMENTS

In this work we made an attempt to understand how a small regulatory network is operating under external stimulus. This stimulus can be, either the output of a larger network where the module is inserted or simply an external signal acting as a trigger mechanism for the action of the module.

For Regulatory Cascades (RC) we have shown that there are two (non exclusive) conditions under which the RC acts as a finite time delayed transducer (or translator) exactly as a cellular automata. It takes a finite input “message” in another finite output “message”. This two conditions are, either an internal property of the module (readable in its parameter

values) or an external characteristic of the input signal. In a sense we can say that under one (or both) of these conditions the module works in a safety operating regime since it can transmit an unambiguous command with only some delay.

In the opposite case, the situation is different since then, in principle, the module needs a variable, eventually infinite, time to “understand” the input message and then to be able to produce an unambiguous output. Moreover this time delay may depend of the particular input signal (see final part of Remark 2.1). No doubt that in this case the module is not of a great help for the system, even if this behavior is fascinating from the point of view of nonlinear dynamics. But maybe Nature has found already somewhere a situation where this fuzzy-like operating regime has some selective advantage!

From a mathematical point of view our strategy was first to prove these properties on the simplest possible module (the elementary transducer ET) and then extend them step by step up to the general case (RC).

For the Forced Circuits (FC) we use a slightly different strategy. In each case we work out the subsets of the phase space involved in the dynamics under each external input. Here the case of stationary inputs enable a simple classification of the different “extreme” dynamical responses of the module. Then thanks to the contracting (or diffusive) properties of the dynamics (a consequence of degradation) we may predict the dynamics under more general inputs. This also opens the possibility to build small modules with different desired functionalities. From a mathematical point of view our strategy was simply to restrict the dynamics in each FC to the part of the phase space that became invariant and attractive under each specific input.

These small open circuits show how their functioning may depend on the parameters as well as on the different type of inputs. In this context, the notion of modularity for the accomplishment of a function cannot be reduced to a simple decomposition of the network into subsets of nodes and interactions.

An example where such ambiguity may be interesting for a biological function is the case where for a while a cell population needs two types of differentiated cells (corresponding to low and medium expression level of genes for instance, see Figure 11 (B), up to a moment when, under an appropriate signal (generated by a stress for instance), the two states switch to the same effective differentiated state (high expression level of genes for instance), see Figure 11 (C).

Now we may wonder why we need one point of view (transducer) when dealing with RC and another (constrained phase space) to study FC. The two points of view are in fact equivalent. The bridge between them is symbolic dynamics. The starting point of symbolic dynamics is to encode the atoms of a suitable partition of the phase space by a set of symbols and to transfer the description of the dynamics in the phase space in terms of rules on the corresponding symbolic representation. In our case the partition of phase space is naturally determined by the set of thresholds and the corresponding symbols by the values of the Heaviside function $H(\sigma(\mathbf{x} - T))$. With this dictionary in mind it is clear that the transducer in the RC case uses the phase space made available by the input signal to encode the message and, *vice-versa*, in the FC each node send to the others a code defined by its position in the available phase space. These are just two faces of the same coin.

Our conclusion is that the existence of open designed dynamical modules leads to an extremely reach set of different dynamical behaviors making such units capable of carrying through various performances in response to different external stimuli. But, on the other hand we have seen that in many cases the same functionality may be performed by different modules. The possible criteria for the selection of a particular module among other displaying the same function open to very interesting questions [18].

The fine tune of the dynamics of a module by a complex input is a current subject of our efforts. As for further research in a connected direction, we mention the interesting problem of reverse engineering, control and bifurcations for such modules that we have just touched in Example 4.1 .

We are still far from a complete understanding of the way how module's architecture, parameters and inputs are related to functionalities in all cases, and *vice-versa*. Nevertheless we are convinced that our results give an insight in the fascinating interplay between modularity and dynamics.

REFERENCES

- [1] C. Aguirre, J. Martins and R. Vilela Mendes, "Dynamics and coding of a biologically motivated network", *International Journal of Bifurcation and Chaos* **16** (2) (2006) 383–394.
- [2] U. Alon, "An Introduction to Systems Biology: Design Principles of Biological Circuits", *Chapman & Hall/CRC/Taylor & Francis*, 2007.
- [3] U. Alon, "Network Motifs: theory and experimental approaches", *Nature* **8** (2007) 450–461.
- [4] L. Arnold, "Random Dynamical Systems", *Springer Verlag* (1995).
- [5] R. Coutinho, "Dinâmica simbólica linear", PhD Thesis, *Technical University of Lisbon* (1999).
- [6] R. Coutinho, B. Fernandez, R. Lima and A. Meyroneinc, "Discrete-time Piecewise Affine Models of Genetic Regulatory Networks", *Journal of Mathematical Biology* **52** (4) (2006) 524–570.
- [7] H. de Jong, "Modeling and simulation of genetic regulatory systems: a literature review", *Journal of Computational Biology* **9** (2002) 67–103.
- [8] H. de Jong and R. Lima, "Modeling the Dynamics of Genetic Regulatory Networks: Continuous and Discrete Approaches" *CML2004 proceedings*, Paris, Springer (2005).
- [9] R. Edwards, H. T. Siegelmann, K. Aziza and L. Glass, "Symbolic dynamics and computation in model gene networks", *Chaos* **11** (2001) 160–169.
- [10] B. M. Elowitz and S. A. Leibler, "A synthetic oscillatory network of transcriptional regulators" *Nature* **403** (2000) 335–338.
- [11] D. Gordon, "On the computational power of totalistic cellular automata", *Mathematical Systems Theory* **20** (1987) 43–52.
- [12] P. J. Ingram, M. P. Stumpf and J. Stark, "Network motifs structure does not determine function", *BMC Genomics* **7** (2006) Paper No. 108.
- [13] A. Isidori, "Nonlinear control systems: An introduction", *Lecture Notes in Control and Information Sciences*, Springer-Verlag (1985).
- [14] R. Lima and E. Ugalde, "Dynamical Complexity of Discrete-time Regulatory Networks", *Nonlinearity* **19** (1) (2006) 237–259.
- [15] K. Lindgren and M. G. Nordahl, "Universal computation in simple one-dimensional cellular automata", *Complex Systems* **4** (1990) 299–318.
- [16] S. Mangan and U. Alon, "Structure and function of the feed-forward loop network motif", *PNAS* **100** (21) (2003) 11980–11985.
- [17] R. Milo, S. Shen-Orr, S. Itzkovitz, N. Kashtan, D. Chklovskii and U. Alon, "Network Motifs: Simple Building Blocks of Complex Networks", *Science* **298** (2002) 824–827.

- [18] M. A. Savageau, “Design of Molecular Control Mechanisms and the Demand for Gene Expression.”, *Proceedings of the National Academy of Sciences* **74** (1977), 5647–5651.
- [19] G. Schlosser and G. P. Wagner (Ed.), “Modularity in Development and Evolution”, *The University of Chicago press* (2004).
- [20] E. Sontag, “Mathematical Control Theory: Deterministic Finite Dimensional Systems”, Second Edition, Springer, New York (1998).
- [21] D. Thieffry, A. M. Huerta, E. Perez–Rueda and J. Collado–Vides, “From specific gene regulation to genomic networks: a global analysis of transcription regulation in *escherichia coli*”, *Bioessays* **20** (2000) 433–440.
- [22] R. Thomas, D. Thieffry and M. Kaufmann, “Dynamical behaviour of biological regulatory networks. I. Biological role of feedback loops and practical use of the concept of the loop–characteristic state”, *Bulletin of Mathematical Biology* **57** (1995) 247–276.
- [23] R. Thomas, “Logical analysis of systems comprising feedback loops”, *Journal Theoretical Biology* **73** (1978) 631–656.
- [24] R. Thomas, “Regulatory networks seen as asynchronous automata: a logical description”, *Journal Theoretical Biology* **153** (1991) 1–23.
- [25] D. Volchenkov and R. Lima, “Random Shuffling of Switching Parameters in a Model of Gene Expression Regulatory Network”, *Stochastics and Dynamics* **5** (1) (2005), 75–95.